

Article

# Robust Underwater Acoustic Channel Estimation Method Based on Bias-Free Convolutional Neural Network

Diya Wang <sup>1,2,3,4</sup> , Yonglin Zhang <sup>1,2</sup>, Lixin Wu <sup>1,2,\*</sup>, Yupeng Tai <sup>1,2</sup>, Haibin Wang <sup>1,2</sup>, Jun Wang <sup>1,2</sup>, Fabrice Meriaudeau <sup>3</sup> and Fan Yang <sup>4</sup> 

<sup>1</sup> State Key Laboratory of Acoustics, Institute of Acoustics, Chinese Academy of Sciences, Beijing 100190, China

<sup>2</sup> University of Chinese Academy of Sciences, Beijing 100049, China

<sup>3</sup> Unité Mixte de Recherche, Institut de Chimie Moléculaire, Centre National de la Recherche Scientifique 6302, Université Bourgogne Franche-Comté, 21078 Dijon, France; fabrice.meriaudeau@u-bourgogne.fr

<sup>4</sup> Laboratoire d'Étude de l'Apprentissage et du Développement, Unité Mixte de Recherche, Centre National de la Recherche Scientifique 5022, Université Bourgogne Franche-Comté, 21078 Dijon, France; fanyang@u-bourgogne.fr

\* Correspondence: wlx@mail.ioa.ac.cn

**Abstract:** In recent years, the study of deep learning techniques for underwater acoustic channel estimation has gained widespread attention. However, existing neural network channel estimation methods often overfit to training dataset noise levels, leading to diminished performance when confronted with new noise levels. In this research, a “bias-free” denoising convolutional neural network (DnCNN) method is proposed for robust underwater acoustic channel estimation. The paper offers a theoretical justification for bias removal and customizes the fundamental DnCNN framework to give a specialized design for channel estimation, referred to as the bias-free complex DnCNN (BF-CDN). It uses least squares channel estimation results as input and employs a CNN model to learn channel characteristics and noise distribution. The proposed method effectively utilizes the temporal correlation inherent in underwater acoustic channels to further enhance estimation performance and robustness. This method adapts to varying noise levels in underwater environments. Experimental results show the robustness of the method under different noise conditions, indicating its potential to improve the accuracy and reliability of channel estimation.

**Keywords:** underwater acoustic communication; channel estimation; bias-free; deep learning; convolutional neural network



**Citation:** Wang, D.; Zhang, Y.; Wu, L.; Tai, Y.; Wang, H.; Wang, J.; Meriaudeau, F.; Yang, F. Robust Underwater Acoustic Channel Estimation Method Based on Bias-Free Convolutional Neural Network. *J. Mar. Sci. Eng.* **2024**, *12*, 134. <https://doi.org/10.3390/jmse12010134>

Academic Editor: Sergej Chernyi

Received: 23 November 2023

Revised: 10 December 2023

Accepted: 30 December 2023

Published: 9 January 2024



**Copyright:** © 2024 by the authors. Licensee MDPI, Basel, Switzerland. This article is an open access article distributed under the terms and conditions of the Creative Commons Attribution (CC BY) license (<https://creativecommons.org/licenses/by/4.0/>).

## 1. Introduction

Underwater acoustic (UWA) communication systems have become a critical component to meet the rising demand for marine exploration and commercial activities. These systems facilitate a diverse set of applications, including oceanographic research, offshore oil and gas exploration, and the Internet of Underwater Things [1–3]. The UWA wave is often regarded as one of the most demanding communication mediums as it is characterized by limited bandwidth, significant multipath spread, fast fading, and intricate oceanic noise [4,5].

Orthogonal frequency division multiplexing (OFDM) for UWA communication has gained substantial attention due to its high spectral efficiency and resistance to long multipath spread in UWA channels [6]. The basic idea behind OFDM is to split the channel bandwidth into evenly spaced subchannels in the frequency domain. Given the challenges posed by frequency-selective fading and substantial noise fluctuations in certain UWA environments, accurate channel estimation is crucial for a UWA OFDM communication system. Traditional channel estimation methods, such as the least squares (LS) estimation algorithm, suffer from poor performance in low signal-to-noise ratio (SNR) conditions, as the estimated mean square error (MSE) is inversely proportional to the SNR. In comparison

to LS estimation, minimum mean square error (MMSE) estimation utilizing second-order statistics of the channel can achieve higher estimation accuracy. However, it requires prior knowledge of noise and channel statistics, and its complexity is much higher than that of LS estimation.

In recent years, machine learning, especially deep learning (DL), has rapidly progressed and been widely applied in various fields, offering new solutions to the challenges in UWA communication [7–9]. Zhang et al. [10] developed a UWA OFDM communication receiver system based on a five-layer fully connected deep neural network (DNN) for UWA channel estimation and equalization. The model demonstrated advantages over traditional algorithms, especially in scenarios with limited pilot subcarriers in OFDM communication. In a subsequent work, Zhang et al. [11] introduced a UWA OFDM communication receiver system utilizing a combination of a convolutional neural network (CNN) for feature extraction and multilayer perceptron (MLP) for data symbol recovery. This model outperforms traditional methods and fully connected DNN-based UWA OFDM frameworks. Liu et al. [12] proposed a CNN-based UWA OFDM receiver system that effectively integrates channel estimation and equalization. The design features an encoder and decoder structure with convolutional layers for feature extraction and signal reconstruction, which reduces network complexity. Qiao et al. [13] introduced CsiPreNet, a learning model comprising a one-dimensional CNN and long short-term memory (LSTM) network. This model captures the temporal and spectral characteristics of UWA channel state information (CSI) and outperforms existing recursive least square (RLS) predictors. Ouyang et al. [14] modified a super-resolution neural network to address the channel estimation problem, resulting in the channel super-resolution network (CSRNet). Simulation results showed superior performance compared to LS. Liu et al. [15] introduced a method for UWA channel estimation based on a denoising sparsity-aware DNN (DeSA-DNN). Their approach uses DNN to simulate the iterative process of classical sparse reconstruction algorithms, leveraging the sparsity of UWA channels. It incorporates an effective denoising module using CNN to mitigate the impact of interference on channel estimation.

In summary, CNN-based methods offer simplicity and flexibility in adapting to the characteristics of UWA channels. However, existing CNN-based channel estimation approaches often focus on single data-block estimations and lack consideration of the temporal correlation within the channel. Moreover, these methods are typically trained within specific SNR ranges, while UWA channels often exhibit significant SNR fluctuations. This can potentially lead to overfitting within the training SNR range and a decrease in performance outside of it.

In this paper, a robust underwater acoustic channel estimation method based on a bias-free CNN is introduced. The main contributions of this research can be summarized as follows:

1. We incorporate the “bias-free” concept [16] into denoising convolutional neural network (DnCNN) enhances the stability of the model performance and aims to overcome overfitting the training SNR conditions. And through theoretical justification and framework customization, we develop a specialized neural network for channel estimation known as bias-free complex DnCNN (BF-CDN).
2. Utilizing the temporal correlation of the channel over a certain time period, the input to the model consists of the coarse channel estimation results of data blocks received within a certain time segment. This results in further improvement and robustness in estimation performance.
3. Simulations and real sea experimental data results confirm the robustness of the method under different noise conditions and highlight its potential to improve the accuracy and reliability of channel estimation.

The rest of this paper is structured as follows: Section 2 provides a brief overview of the UWA-OFDM system model. Section 3 introduces the proposed BF-CDN model for channel estimation and covers the problem transformation, theoretical explanation, and

model architecture design. Section 4 presents simulation and experimental results and provides an analysis of these findings. Finally, in Section 5, we conclude the paper.

## 2. UWA-OFDM System Model

Assume that  $\mathbf{h}(n)$  represents the UWA channel

$$\mathbf{h}(n) = \sum_{i=1}^N A_i(n)\delta(\tau - \tau_i(n)). \tag{1}$$

The UWA channel is assumed to be approximated by  $N$  dominant discrete paths, where each path is associated with a complex gain  $A_i(n)$  and time delay  $\tau_i(n)$  at the  $i$ -th discrete sample time. The formation of multipath in UWA channels is a result of various factors, including reflection on the water’s surface, seafloor, and object surfaces as well as refraction in water. These factors collectively contribute to the time-varying nature of UWA channels.

We consider a cyclic prefix (CP) OFDM baseband system in this context. The block diagram of the system is shown in Figure 1. After passing through the channel, the signal obtained by the receiver can be expressed as

$$\mathbf{y}(n) = \mathbf{x}(n) \otimes \mathbf{h}(n) + \mathbf{w}(n), \tag{2}$$

where  $\otimes$  represents the circular convolution, and  $\mathbf{x}(n)$  and  $\mathbf{w}(n)$  denote the transmitted signal and additive noise, respectively. After removing the CP, the received signal in the frequency domain can be obtained by DFT transformation:

$$\mathbf{Y} = \text{diag}(\mathbf{X})\mathbf{F}\mathbf{h} + \mathbf{W}, \tag{3}$$

where  $\text{diag}(\mathbf{X})$  is the diagonal matrix of the transmitted symbols,  $\mathbf{F}$  is the corresponding Fourier transform matrix,  $\mathbf{h}$  is the time domain channel, and  $\mathbf{Y}$  and  $\mathbf{W}$  denote the frequency domains of  $\mathbf{y}(n)$  and  $\mathbf{w}(n)$ , respectively.

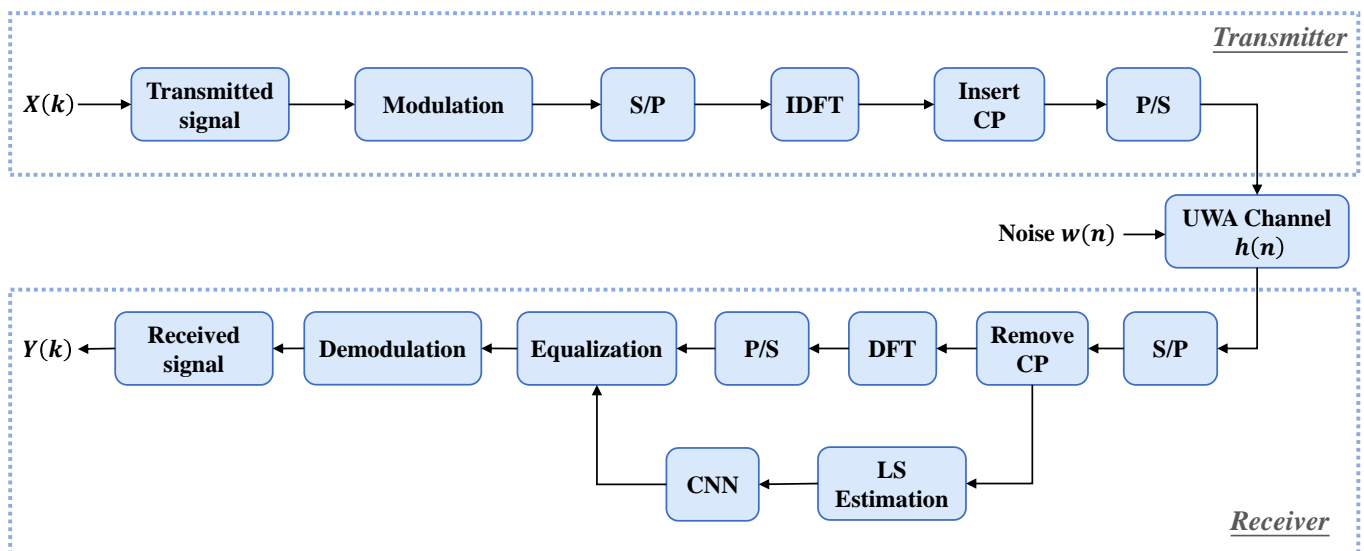


Figure 1. The considered CNN-based UWA-OFDM system architecture.

## 3. Methods

### 3.1. Problem Transformation

In traditional DL-based UWA channel estimation methods, several approaches, such as [10,11,17], employ model inputs consisting of received symbols and transmitted pilots. This type of input often requires keeping the pilot symbols fixed during the training phase, leading to strong coupling between the model parameters and the transmitted symbols, which is not conducive to transferability. Therefore, in our approach, we utilize the coarse

channel estimation results as the model input. To reduce computational complexity, we employ the LS estimator.

In traditional UWA-OFDM systems, pilots are extracted and used for channel estimation. Assume that the pilots are equispaced; the LS solution in time domain can be expressed as [18]

$$\hat{\mathbf{h}}_{LS}(n) = \frac{1}{K_p} \mathbf{F}_p^H \text{diag}(\mathbf{X}_p)^H \mathbf{Y}_p, \tag{4}$$

where  $K_p$  is the number of pilots,  $\mathbf{Y}_p$  is a  $K_p \times 1$  vector that consists of the received pilot symbols,  $\text{diag}(\mathbf{X}_p)$  is the  $K_p \times K_p$  diagonal matrix with the known pilot positions along its diagonal, and  $\mathbf{F}_p$  represents the  $K_p \times N$  DFT matrix. The MSE of the LS estimator is calculated as [19,20]

$$\mathcal{D}_{LS} = \mathbb{E} \left\| \hat{\mathbf{h}}_{LS}(n) - \mathbf{h}(n) \right\|_2^2 = \mathbb{E} \left\{ \frac{\mathbf{w}(n)^2}{\mathbf{x}_p(n)^2} \right\} = \frac{1}{\sigma_x^2 / \sigma_w^2}, \tag{5}$$

where  $\mathbf{x}_p(n)$  represents the transmitted pilot signal. This formula demonstrates that the MSE of the LS estimation is inversely proportional to the SNR, where  $\sigma_w^2$  and  $\sigma_x^2$  represent the variances of the pilots and the noise, respectively. Assuming the LS channel estimation results as the model input, with the goal to approximate the true UWA channel, the model output can be represented as

$$\hat{\mathbf{h}}_{\text{output}} = \mathcal{F}(\hat{\mathbf{h}}_{LS}(n); \theta), \tag{6}$$

where  $\theta \triangleq \{\theta_l\}_{l=1}^L \triangleq \{w_l, b_l\}_{l=1}^L$  represents the training parameters in the neural network,  $L$  represents the number of network layers,  $w_l$  and  $b_l$  denote the weight items and bias items of the  $l$ -th layer, respectively, and  $\mathcal{F}(\cdot)$  represents the forward computation of the model.

If the MSE is assumed as the training loss function, then

$$\mathcal{L}(\Theta) = \frac{1}{M_{\text{tr}}} \sum_{m=1}^{M_{\text{tr}}} \left\| \mathbf{h}(n)^m - \mathcal{F}(\hat{\mathbf{h}}_{LS}(n)^m; \theta) \right\|_2^2 \propto \frac{1}{\text{SNR}}, \tag{7}$$

where  $M_{\text{tr}}$  is the batch size, and  $\propto$  is defined as ‘‘is proportional to’’. Based on the analysis of the aforementioned issues, the LS channel estimation problem shares similarities with image denoising. Specifically, it involves removing noise impact on estimation results. Leveraging this insight, this paper applies DL denoising techniques to address the channel estimation problem.

Among DL-based image denoising methods, DnCNN [21] is one of the most representative approaches. Building upon this foundation, this paper adopts and modifies the fundamental framework of DnCNN to design a channel estimation neural network.

### 3.2. Theoretical Analysis of DnCNN Estimator

UWA channels often exhibit significant SNR variations, and traditional neural network channel estimation methods tend to overfit within specific SNR ranges, leading to performance degradation outside the training SNR. To address this challenge, we apply the bias-free concept, which was initially introduced and validated for its robustness to SNR variations in image denoising [16], to the field of UWA channel estimation. Furthermore, we provide an explanation of why bias-free is relevant to channel estimation.

Under the criterion of minimizing MSE, MMSE estimation is optimal, and it can be expressed as [22]

$$\hat{\mathbf{h}}_{MMSE}(n) = \mathbf{r}_{\text{hh}} \left( \mathbf{r}_{\text{hh}} + \frac{\sigma_w^2}{\sigma_x^2} \mathbf{I}_d \right)^{-1} \hat{\mathbf{h}}_{LS}(n), \tag{8}$$

where  $\mathbf{r}_{\mathbf{h}\mathbf{h}} = E[\mathbf{h}(n)\mathbf{h}(n)^H]$  refers to the autocorrelation matrix of the channel vector  $\mathbf{h}(n)$  in the time domain, and  $\mathbf{I}_d$  denotes the identity matrix. The MSE of the MMSE estimator can be expressed as [23]

$$\mathcal{D}_{MMSE} = \mathbb{E}\left\{\|\hat{\mathbf{h}}_{MMSE}(n) - \mathbf{h}(n)\|_2^2\right\} = tr\left\{\mathbf{r}_{\mathbf{h}\mathbf{h}}\left(\frac{\sigma_w^2}{\sigma_x^2}\mathbf{r}_{\mathbf{h}\mathbf{h}} + \mathbf{I}_d\right)^{-1}\right\} \leq \mathcal{D}_{LS}, \quad (9)$$

where  $tr$  represents the trace of a matrix.

In Equation (6), the function  $\mathcal{F}$  computed by a DnCNN can be expressed as

$$\begin{aligned} \hat{\mathbf{h}}_{DnCNN}(n) &= \mathcal{F}(\hat{\mathbf{h}}_{LS}(n)) \\ &= w_L \cdot R(w_{L-1} \cdot \dots \cdot R(w_1 \cdot \hat{\mathbf{h}}_{LS}(n) + b_1) + \dots + b_{L-1}) + b_L \\ &= A_h \hat{\mathbf{h}}_{LS}(n) + b_h, \end{aligned} \quad (10)$$

where  $w_L$  to  $w_1$  are the weight items of the neural network,  $R$  represents the activation function rectified linear unit (ReLU), and  $b_L$  to  $b_1$  are the bias terms. The matrix  $A_h$  serves as the equivalent of the overall weight matrix of the network, and vector  $b_h$  plays an equivalent role to the overall bias of the network. As the error vector of the optimal estimator (in terms of MSE)  $[\hat{\mathbf{h}}_{MMSE}(n) - \mathbf{h}(n)]$  is orthogonal to any possible estimator [24], we can express the MSE of the DnCNN estimator as [20]

$$\begin{aligned} \mathcal{D}_{DnCNN} &= \mathbb{E}\left\{\|\hat{\mathbf{h}}_{DnCNN}(n) - \mathbf{h}(n)\|_2^2\right\} \\ &= \mathbb{E}\left\{\|\hat{\mathbf{h}}_{DnCNN}(n) - \hat{\mathbf{h}}_{MMSE}(n) + \hat{\mathbf{h}}_{MMSE}(n) - \mathbf{h}(n)\|_2^2\right\} \\ &= \mathbb{E}\left\{\|\hat{\mathbf{h}}_{DnCNN}(n) - \mathbf{h}_{MMSE}(n)\|_2^2\right\} + \mathbb{E}\left\{\|\hat{\mathbf{h}}_{MMSE}(n) - \mathbf{h}(n)\|_2^2\right\} \\ &\quad + 2\mathbb{E}\left\{(\hat{\mathbf{h}}_{DnCNN}(n) - \mathbf{h}_{MMSE}(n))^H(\hat{\mathbf{h}}_{MMSE}(n) - \mathbf{h}(n))\right\} \\ &= \mathbb{E}\left\{\|\hat{\mathbf{h}}_{DnCNN}(n) - \hat{\mathbf{h}}_{MMSE}(n)\|_2^2\right\} + \mathcal{D}_{MMSE}. \end{aligned} \quad (11)$$

Substituting Equations (8) and (10) into Equation (11) results in

$$\begin{aligned} \mathcal{D}_{DnCNN} &= \mathbb{E}\left\{\|\hat{\mathbf{h}}_{DnCNN}(n) - \hat{\mathbf{h}}_{MMSE}(n)\|_2^2\right\} + \mathcal{D}_{MMSE} \\ &= \mathbb{E}\left\{\|A_h \hat{\mathbf{h}}_{LS}(n) + b_h - \mathbf{r}_{\mathbf{h}\mathbf{h}}\left(\mathbf{r}_{\mathbf{h}\mathbf{h}} + \frac{\sigma_w^2}{\sigma_x^2}\mathbf{I}_d\right)^{-1}\hat{\mathbf{h}}_{LS}(n)\|_2^2\right\} + \mathcal{D}_{MMSE}. \end{aligned} \quad (12)$$

Next, let us represent  $\mathbf{r}_{\mathbf{h}\mathbf{h}}(\mathbf{r}_{\mathbf{h}\mathbf{h}} + \frac{\sigma_w^2}{\sigma_x^2}\mathbf{I}_d)^{-1}$  as  $A_{MMSE}$ ; we can restate  $\mathcal{D}_{DnCNN}$  as

$$\mathcal{D}_{DnCNN} = \mathbb{E}\left\{\|A_h \hat{\mathbf{h}}_{LS}(n) + b_h - A_{MMSE} \hat{\mathbf{h}}_{LS}(n)\|_2^2\right\} + \mathcal{D}_{MMSE}. \quad (13)$$

It can be observed that  $A_{MMSE}$  represents a linear transformation.  $A_h$  serves as the weight matrix for the DnCNN estimator and aims to approximate  $A_{MMSE}$  to minimize the MSE. Notably, the presence of  $b_h$  does not contribute to minimizing the MSE. Therefore, it can be omitted to prevent overfitting.

Therefore, the performance comparison among the aforementioned methods can be outlined as follows:

$$\mathcal{D}_{LS} \geq \mathcal{D}_{DnCNN} \approx \mathcal{D}_{MMSE}. \quad (14)$$

### 3.3. Proposed BF-CDN Architecture

Beyond the bias removal requirement discussed earlier, channel estimation differs from image denoising in two significant ways. (1) Complex vs. real values: While image denoising deals with real-value inputs in three-channel RGB matrices, channel estimation involves complex values. (2) One-dimensional vs. two-dimensional: Images are two-dimensional matrices and are typically processed using two-dimensional convolutions. In channel estimation, the results are represented as one-dimensional vectors.

Due to these differences, this paper employs one-dimensional complex convolution layers (ComplexConv1d) to effectively leverage complex values in UWA channel estimation. The complex convolution layer can be represented as [25]

$$\begin{bmatrix} \Re(x^{OUT}) \\ \Im(x^{OUT}) \end{bmatrix} = \begin{bmatrix} A & -B \\ B & A \end{bmatrix} \begin{bmatrix} \Re(x^{IN}) \\ \Im(x^{IN}) \end{bmatrix}, \quad (15)$$

where  $x^{IN}$  and  $x^{OUT}$  represent the input and output of the network layer, respectively,  $\Re(\cdot)$  and  $\Im(\cdot)$  are responsible for extracting the real and imaginary parts, respectively, and  $A$  and  $B$  are the real and imaginary parts, respectively, of a complex kernel  $w = A + iB$ . Furthermore, a complex activation function, ComplexReLU, is utilized in this context; it is defined as [26]

$$\text{ComplexReLU}(x^{OUT}) = \text{ReLU}(\Re(x^{OUT})) + i * \text{ReLU}(\Im(x^{OUT})). \quad (16)$$

Based on the optimizations of and modifications to the basic DnCNN as described above, we obtain a BF-CDN architecture suitable for UWA-OFDM channel estimation.

As shown in Figure 2, for a given depth of BF-CDN, there are three types of layers: (i) For the first layer, a ComplexConv1d and ComplexReLU are employed. The input feature map has a dimension corresponding to the length of the LS estimation results. (ii) For the hidden layers, batch normalization (BN) is added after the ComplexConv1d, and the number of features in the hidden layers remains unchanged; these are followed by a ComplexReLU. (iii) For the last layer, a ComplexConv1d is used to restore the number of features to the size of the channel dimension.

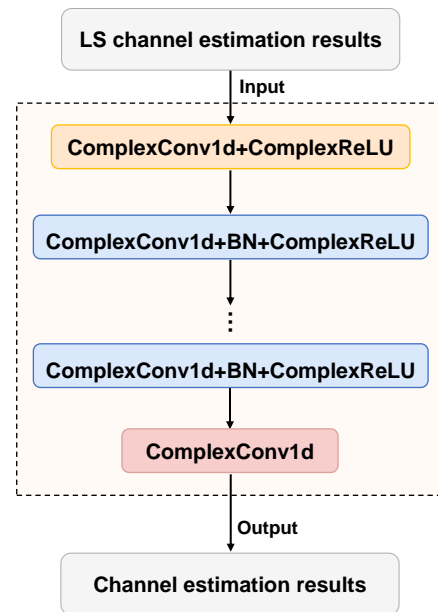


Figure 2. The architecture of BF-CDN.

It is worth noting that the bias terms are removed in each convolutional layers to mitigate overfitting; this architecture can be represented as follows:

$$\begin{aligned} \hat{\mathbf{h}}_{BF-CDN}(n) &= \mathcal{F}(\hat{\mathbf{h}}_{LS}(n)) \\ &= w_L \cdot R(w_{L-1} \cdot \dots \cdot R(w_1 \cdot \hat{\mathbf{h}}_{LS}(n))) \\ &= A_h \hat{\mathbf{h}}_{LS}(n). \end{aligned} \quad (17)$$

Meanwhile, the bias terms are also removed from the BN used during training. On the other hand, UWA channels are typical time-varying channels, and several studies have shown their strong temporal correlation at time scales within the channel coherence time [27,28]. Therefore, the temporal correlation of the channel can be utilized to improve

the performance of channel estimation. Thus, we utilize LS channel estimation results within the channel coherent time as inputs. LS channel estimation results from distinct data blocks are employed as different channel inputs for the model. This approach allows the model to leverage temporal correlations to distinguish between the channel and additive noise more effectively, thereby better extracting the characteristics of the channel.

As described in Equation (7), the model employs MSE as the loss function and utilizes the Adam optimizer.

#### 4. Results and Discussion

##### 4.1. Simulations

To ensure the reliability of the simulations, the channel impulse responses (CIRs) from the real sea UWA communication experiment are used. These CIRs are subjected to manual denoising and then employed as the training and testing datasets for the model. Details about the experiment are presented in Section 4.2.

A total of 700 CIRs were used for the simulations, with 535 CIRs allocated for the training dataset and 135 CIRs for the testing dataset. Other simulation parameters are provided in Table 1. Additional system parameters are provided in Table 2. The model is implemented using the PyTorch framework, while Python serves as the simulation platform. The flow graph of the model is presented in Table 3.

**Table 1.** Parameters of UWA communication simulation.

Parameter	Value
UWA modulation scheme	OFDM with 4QAM
Bandwidth	100 Hz
Center frequency	300 Hz
Number of subcarriers	256
Number of pilots	64
Number of data subcarriers	192
Length of cyclic prefix	0.44 s
Number of blocks in a frame	10

**Table 2.** Other system parameters.

Parameter	Value
Optimizer	Adam
Learning rate	$1 \times 10^{-4}$
Batch number	20
Epoch number	500

**Table 3.** Flow graph of the proposed model.

Layer *	Input Layer	Operation	Output Shape
Input	-	-	(20, 160, 10)
Conv1	ComplexConv1d layer (256, 7, 1, 3)	ComplexReLU	(20, 160, 256)
Conv2	ComplexConv1d layer (256, 7, 1, 3)	BN + ComplexReLU	(20, 160, 256)
Conv3	ComplexConv1d layer (256, 7, 1, 3)	BN + ComplexReLU	(20, 160, 256)
Conv4	ComplexConv1d layer (256, 7, 1, 3)	BN + ComplexReLU	(20, 160, 256)
Output	ComplexConv1d layer (10, 7, 1, 3)	-	(20, 160, 10)

\* The convolutional layer (C, K, stride, padding). C: channel number, K: kernel size, stride: stride of the convolution, padding: padding added to both sides of the input.

##### 4.1.1. Robustness under Various Noise Levels

To evaluate the robustness of the proposed method under various noise levels for UWA channel estimation, we first compare the performance between DnCNN and BF-CDN.

In Figure 3, we depict the average error levels on the test set for both methods across different training SNR ranges. It is observed that within their respective training SNR

ranges, DnCNN performs well. However, when subjected to new noise levels, it experiences a substantial decline in performance, revealing evident overfitting issues within the model-training noise level. In contrast, BF-CDN maintains relatively stable performance outside the training range, even when faced with different noise conditions.

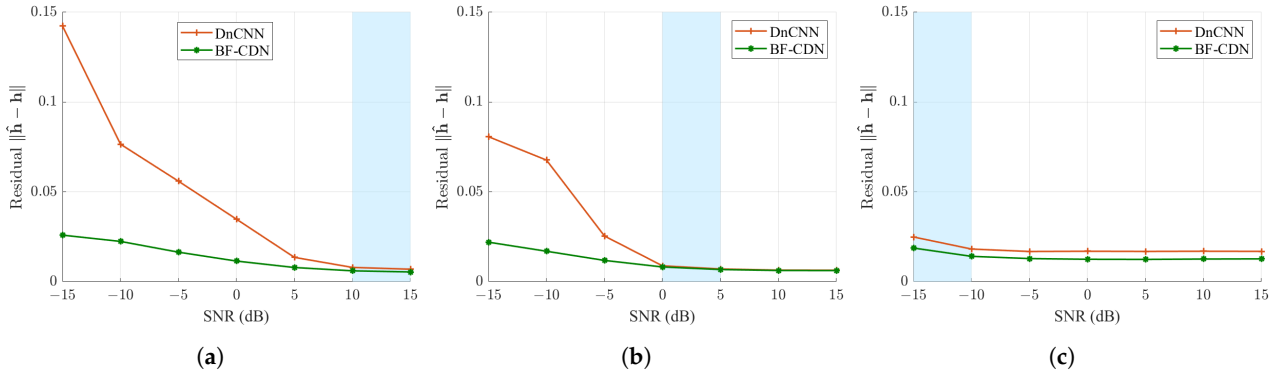


**Figure 3.** The residual norms of the estimated channels and the true channels within different training SNR ranges. The training SNR ranges are highlighted in the blue area: (a) SNR  $\in [10, 15]$  dB, (b) SNR  $\in [0, 5]$  dB, and (c) SNR  $\in [-10, -15]$  dB.

For a more intuitive explanation, a comparison of channel estimation results is provided for scenarios outside the training SNR range. Channel estimation results of three samples are shown by using DnCNN and BF-CDN models, with both models trained within an SNR range of 10 to 15 dB. In Figure 4, with a testing SNR of 15 dB, it is evident that within the training SNR range, both DnCNN and BF-CDN exhibit excellent performance, accurately estimating the channel conditions. Conversely, in Figure 5, with a testing SNR of  $-10$  dB, DnCNN exhibits poor performance. By comparison, BF-CDN demonstrates a significant improvement in performance, highlighting the enhanced robustness of the BF-CDN model across different noise conditions.

#### 4.1.2. Gains from Temporal Correlation

Traditional DL-based UWA channel estimation typically adopts estimating individual data blocks to capture static channel characteristics while often overlooking the common temporal correlation gains inherent in UWA channels. For the time-varying channel of several consecutive OFDM blocks within the channel coherence time, the positions of non-zero delays are similar, and the corresponding gains exhibit temporal correlation. Building upon the orthogonal matching pursuit (OMP) algorithm for UWA channel estimation [28], Zhou et al. [29] introduced the simultaneous orthogonal matching pursuit (SOMP) algorithm, which takes into account the temporal correlation between multiple channels. Experimental results have demonstrated promising performance with this method. In this context, we leverage this characteristic to improve the performance of DL-based UWA channel estimation. We provide a comparative analysis with the performance of the SOMP algorithm in Sections 4.1.3 and 4.2.

In this context, based on the BF-CDN framework, a performance comparison is conducted between using LS channel estimation of individual data blocks and using LS channel estimation of 10 data blocks as model inputs (joint estimation, i.e., BF-CDN). Figure 6 illustrates the channel estimation performance of both methods within different training SNR ranges of the test set. It can be observed that, compared to BF-CDN-individual estimation, BF-CDN exhibits smaller estimation errors and more stable performance under various SNR conditions. Furthermore, Figure 7 illustrates examples at an SNR of 15 dB. It is evident that under conditions of high SNR, both BF-CDN-individual and BF-CDN achieve accurate channel estimation. However, as depicted in Figure 8, when the SNR decreases to  $-10$  dB, the estimation performance of BF-CDN-individual significantly underperforms, indicating a weakened ability to suppress noise. In contrast, BF-CDN demonstrates more

precise estimation under the same conditions. This demonstrates that by employing joint estimation with multiple channels over the channel coherence time, the method can capture more channel information and suppress noise effectively, leading to improved channel estimation accuracy.

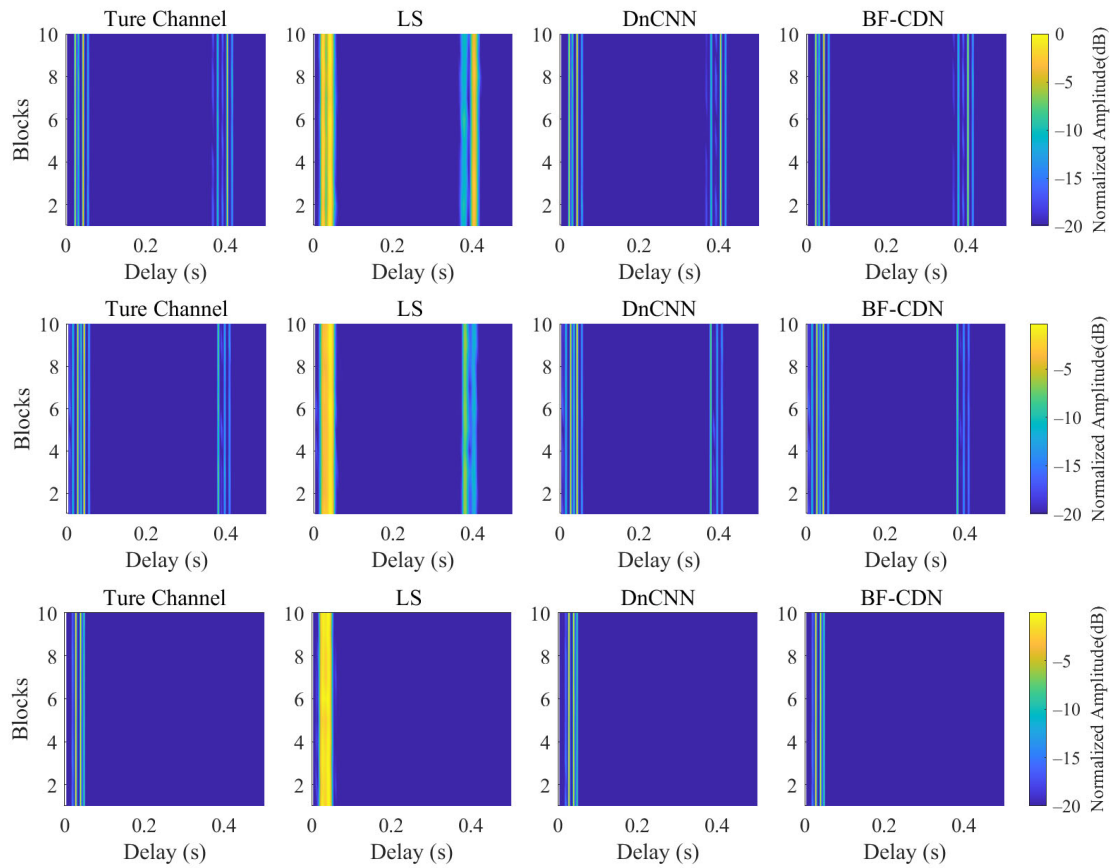


**Figure 4.** Examples of channel estimation results for DnCNN and BF-CDN, with both trained at noise level  $SNR \in [10, 15]$  dB and tested at  $SNR = 15$  dB.

#### 4.1.3. UWA Channel Estimation Performance

In order to assess the channel estimation performance of the proposed method, several commonly used channel estimation methods were compared in simulations. The compared methods include the LS method, the OMP method, the SOMP method, and the condition of known CSI. The LS method serves as the foundational approach for channel estimation, while OMP has been widely adopted as an advanced method in recent years and demonstrates superior performance according to various studies. SOMP, building upon OMP, similarly leverages temporal correlation. Hence, these methods are selected as comparative benchmarks.

The real-time performance of the methods is summarized in Table 4. Simulations were conducted on a computer equipped with an Intel Core i7 CPU operating at 2.50 GHz and with 16 GB of memory. In terms of computational complexity, the DL-based algorithm undergoes a two-phase process involving offline training and online deployment. Following offline training, the model parameters remain constant. During the subsequent online deployment phase, channel estimation is executed through forward propagation using the pre-trained DL model.

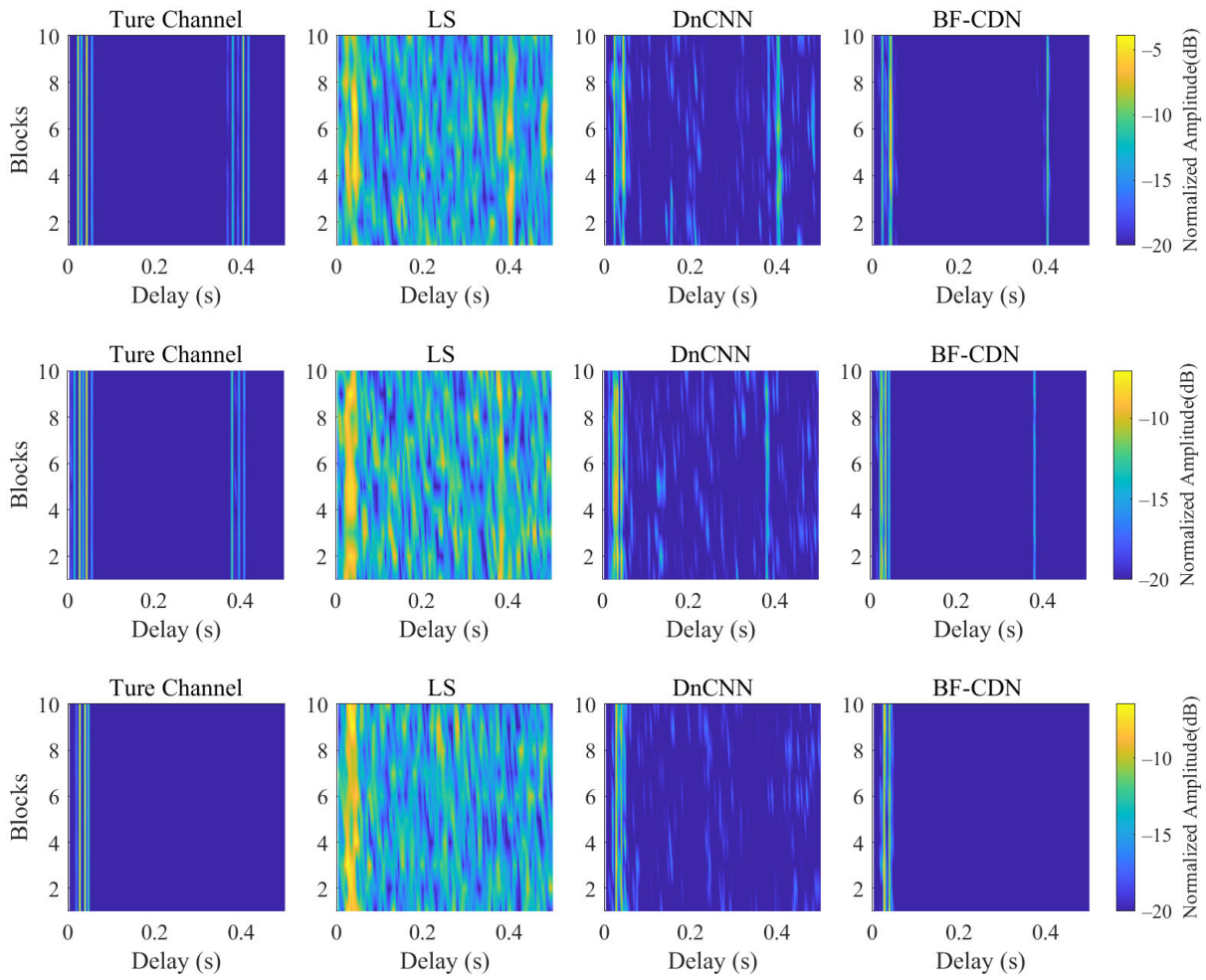


**Figure 5.** Examples of channel estimation results for DnCNN and BF-CDN, with both trained at noise level  $\text{SNR} \in [10, 15]$  dB and tested at  $\text{SNR} = -10$  dB.

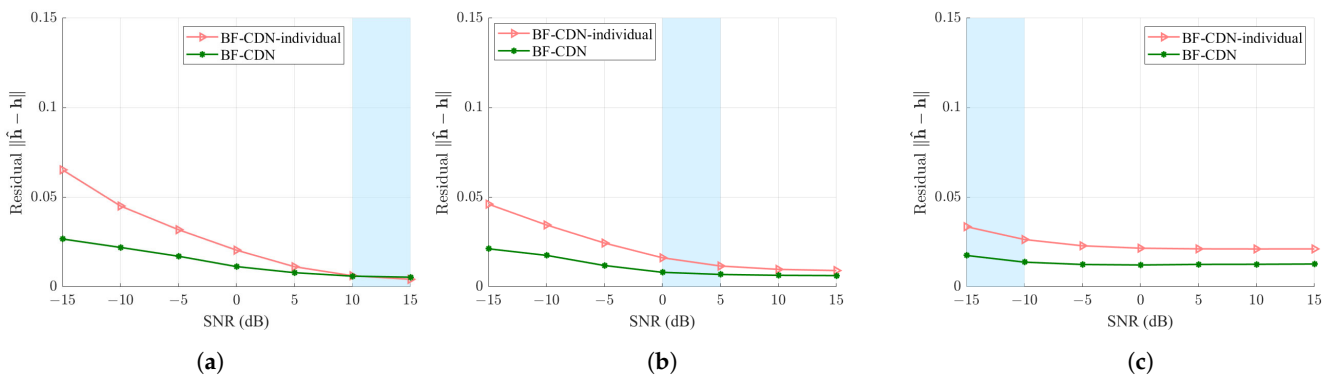


**Figure 6.** The residual norms of the estimated channels and the true channels within different training SNR ranges. The training SNR ranges are highlighted in the blue area: (a)  $\text{SNR} \in [10, 15]$  dB, (b)  $\text{SNR} \in [0, 5]$  dB, and (c)  $\text{SNR} \in [-10, -15]$  dB.

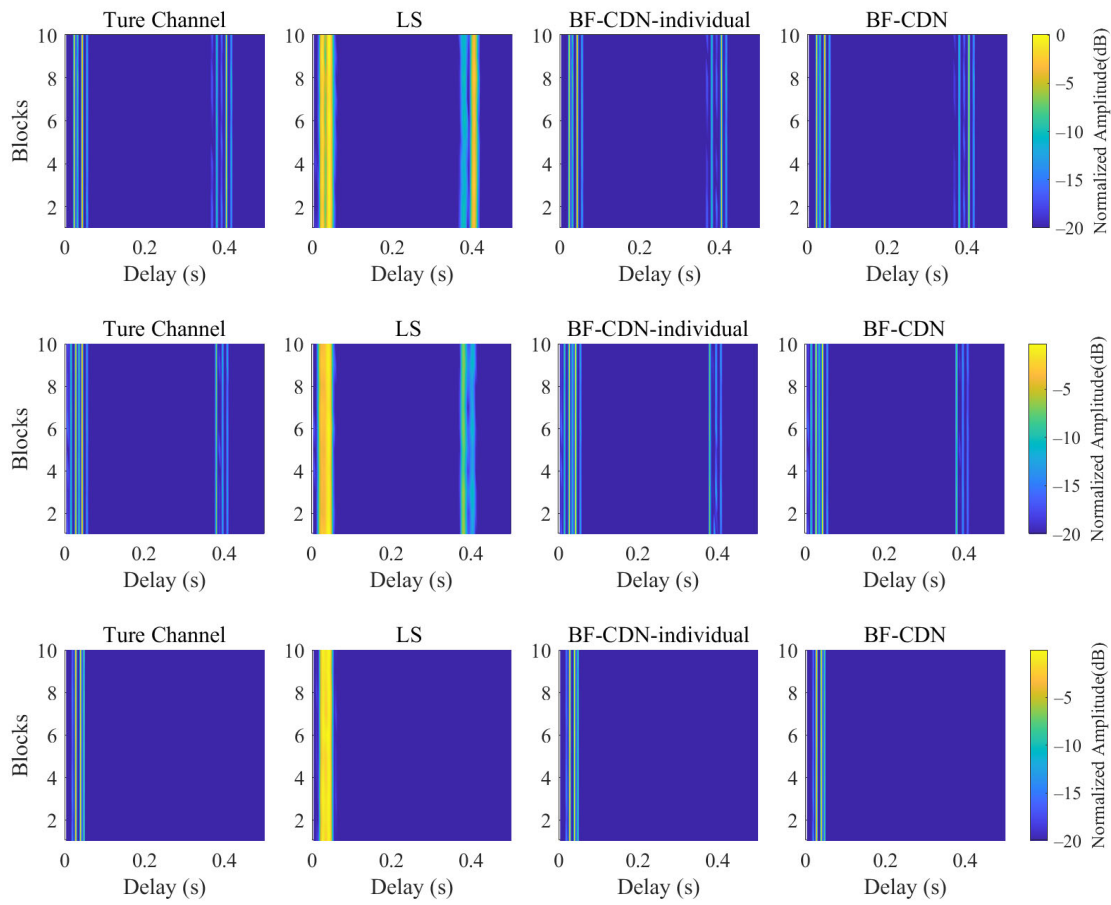


**Figure 7.** Examples of channel estimation results for BF-CDN-individual estimation and BF-CDN, with both trained at noise level  $SNR \in [10, 15]$  dB and tested at  $SNR = 15$  dB.

**Table 4.** Real-time performances of different methods.

Algorithm	Runtime (ms)
LS	3.7
OMP	304.0
SOMP	170.6
DnCNN	16.3
BF-CDN	17.4

Figures 9 and 10 depict the average MSE and bit error rate (BER) performance of the channel test set. It is evident that compared to the LS, OMP, and SOMP algorithms, the proposed method, BF-CDN, significantly reduces channel estimation errors. At an SNR of 15 dB, the MSE performance improvement is 13.8 dB, 7.9 dB, and 7.3 dB, respectively. Furthermore, it consistently maintains optimal BER performance within the SNR of  $[-15 \text{ dB}, 15 \text{ dB}]$ . Correspondingly, the spectral efficiency under various SNRs is presented in Figure 11. It is evident that the proposed method closely approximates the spectral efficiency of the known CSI, demonstrating its efficacy at channel estimation.

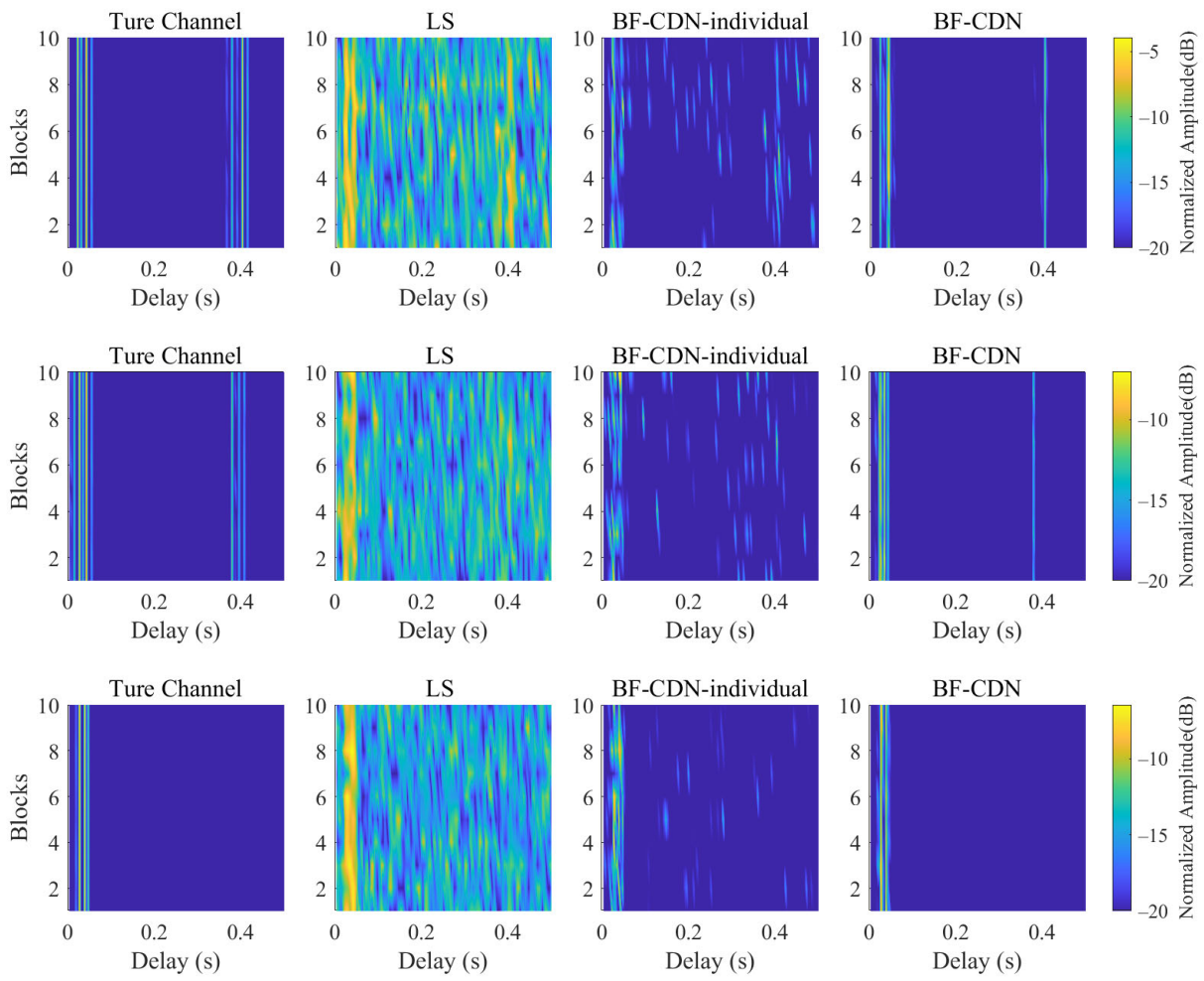


**Figure 8.** Examples of channel estimation results for BF-CDN-individual estimation and BF-CDN, with both trained at noise level  $\text{SNR} \in [10, 15]$  dB and tested at  $\text{SNR} = -10$  dB.

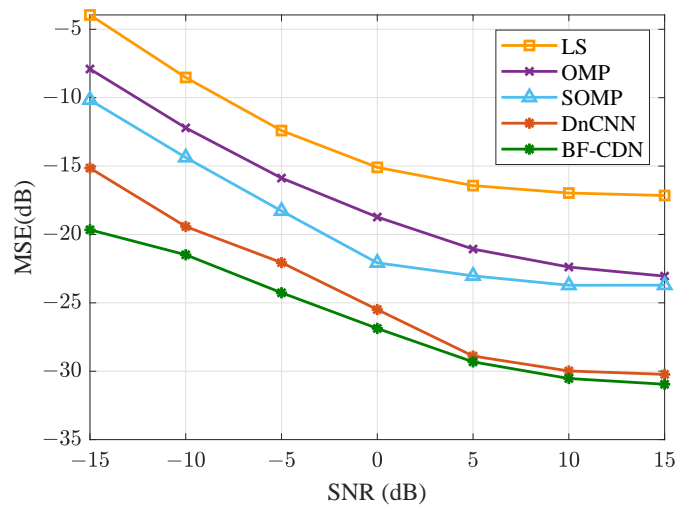


**Figure 9.** The MSE performance on the test set.

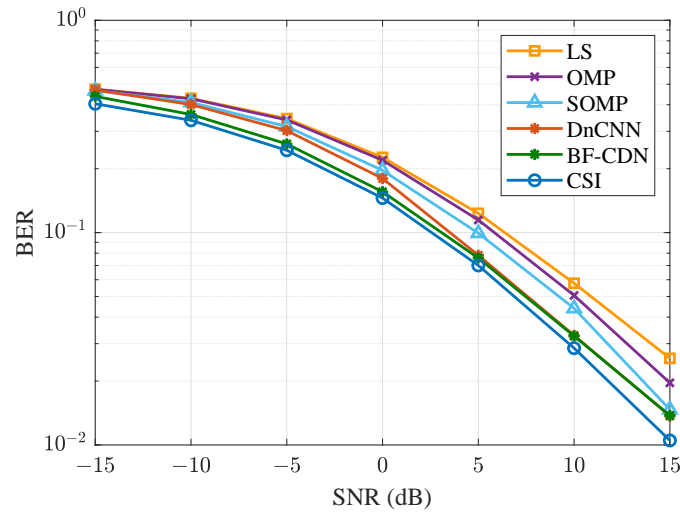


Figure 10. The BER performance on the test set.

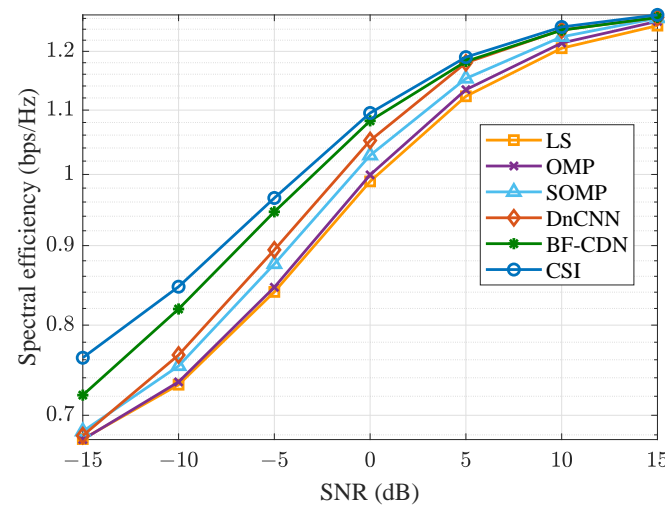


Figure 11. The spectral efficiency on the test set.

#### 4.2. Processing of Real Experimental Data

In this section, we utilized real-world sea trial data to validate the proposed method’s performance. The experiments were conducted in the western Pacific Ocean with fixed positions for both the transmitter and receiver, which were spaced approximately 55 to 60 km apart (with additional distance due to sensors and boats floating). The hydrophone was positioned at a depth of approximately 1040 m underwater. The experimental setup is depicted in Figure 12, while the sound speed profile near the hydrophone is illustrated in Figure 13. Additional experimental parameters are detailed in Table 5.

Table 5. Parameters for UWA communication in real trial.

Parameter	Value
UWA modulation scheme	OFDM with 4QAM
Bandwidth	100 Hz
Center frequency	300 Hz
Number of subcarriers	256
Number of pilots	64
Number of null subcarriers	9
Number of data subcarriers	183
Length of cyclic prefix	0.44 s
Number of blocks in a frame	10

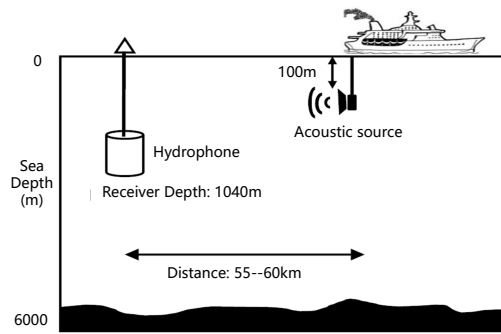


Figure 12. The environment of the seal trail.

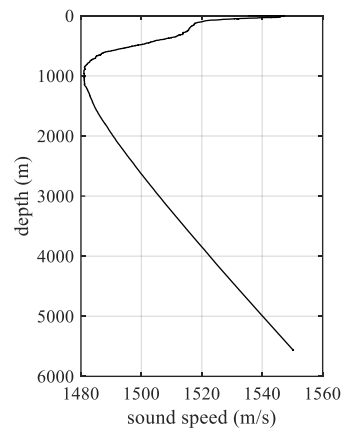


Figure 13. Sound speed profile.

A comparison of channel estimation results for 20 consecutive received OFDM frames is presented in Figure 14, and the corresponding received SNRs are shown in Figure 15. It can be observed that in comparison to LS, OMP, and SOMP, the proposed method consistently maintains superior BER performance under different SNR conditions, demonstrating its excellent robustness for noise fluctuations.

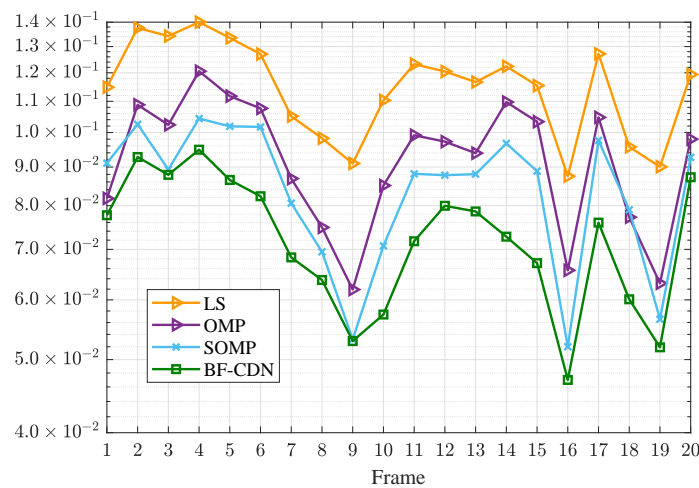
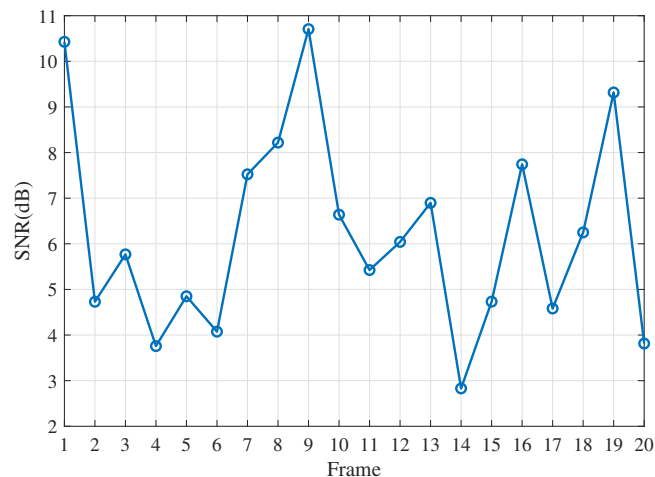


Figure 14. BER performances on sea trial data.



**Figure 15.** The SNR for each received frame in sea trial.

## 5. Conclusions

In this paper, a robust UWA channel estimation method based on the bias-free CNN is introduced. Initially, the LS channel estimation results are employed as a channel affected by noise, and a denoising neural network is applied to achieve accurate channel estimation. Subsequently, the bias-free concept is introduced, and its necessity is theoretically explained and validated through simulations. Then, modifications are made to the model to adapt it for channel estimation. Compared to the DnCNN network, the proposed method exhibits superior robustness for noise fluctuations: even those not encountered during training. Furthermore, simulations confirm that joint estimation further improves the performance and robustness compared to individual estimation by leveraging the temporal correlation of the channel.

Finally, a performance comparison is conducted between the proposed method and classical methods such as LS, OMP, and SOMP. The simulation results show that the method outperforms these classical methods across different SNR levels. At an SNR of 15 dB, the MSE performance improvement is 13.8 dB, 7.9 dB, and 7.3 dB, respectively. Real sea trail data processing further validates the superior performance of the proposed method. In future work, exploration will be conducted on the impact of implementing the bias-free technique within various CNN architectures on channel estimation. The objective is to design and refine models for enhanced performance.

**Author Contributions:** D.W.: methodology, software, investigation, and writing—original draft preparation; Y.Z.: formal analysis, validation, funding acquisition, and writing—review and editing; L.W.: investigation, project administration, resources, and supervision; Y.T.: data curation, formal analysis, project administration, and writing—review and editing; H.W.: data curation, funding acquisition, investigation, and project administration; J.W.: data curation, resources, investigation, and project administration; F.M.: conceptualization, formal analysis, supervision, and writing—review and editing; F.Y.: conceptualization, formal analysis, supervision, and writing—review and editing. All authors have read and agreed to the published version of the manuscript.

**Funding:** This research was supported by the China Scholarship Council, Chinese Academy of Sciences, CAS Specific Research Assistant Funding Program, and the National Natural Science Foundation of China (grant No. 62301551).

**Institutional Review Board Statement:** Not applicable.

**Informed Consent Statement:** Not applicable.

**Data Availability Statement:** The data that support the findings of this study are available from the Institute of Acoustics of the Chinese Academy of Sciences. Restrictions apply to the availability of these data, which were used under license for this study. Data are available from the authors upon

reasonable request and with the permission of the Institute of Acoustics of the Chinese Academy of Sciences.

**Acknowledgments:** The authors would like to thank the editors and reviewers for their comments on the manuscript of this article.

**Conflicts of Interest:** The authors declare no conflicts of interest.

### Abbreviations

The following abbreviations are used in this manuscript:

UWA	Underwater acoustic
OFDM	Orthogonal frequency division multiplexing
LS	Least squares
SNR	Signal-to-noise ratio
MSE	Mean square error
MMSE	Minimum mean square error
DL	Deep learning
DNN	Deep neural network
CNN	Convolutional neural network
MLP	Multilayer perceptron
LSTM	Long short-term memory
CSI	Channel state information
RLS	Recursive least square
CSRNet	Channel super-resolution network
DeSA-DNN	Denosing sparsity-aware DNN
DnCNN	Denosing convolutional neural network
BF-CDN	Bias-free complex denosing convolutional neural network
CP	Cyclic prefix
ReLU	Rectified linear unit
ComplexReLU	Complex rectified linear unit
ComplexConv1d	One-dimensional complex convolution layers
BN	Batch normalization
CIRs	Channel impulse responses
OMP	Orthogonal matching pursuit
SOMP	Simultaneous orthogonal matching pursuit
BER	Bit error rate

### References

1. Stojanovic, M.; Beaujean, P.P.J. Acoustic communication. In *Springer Handbook of Ocean Engineering*; Springer: Cham, Switzerland, 2016; pp. 359–386.
2. Howe, B.M.; Miksis-Olds, J.; Rehm, E.; Sagen, H.; Worcester, P.F.; Haralabus, G. Observing the oceans acoustically. *Front. Mar. Sci.* **2019**, *6*, 426. [\[CrossRef\]](#)
3. Mohsan, S.A.H.; Li, Y.; Sadiq, M.; Liang, J.; Khan, M.A. Recent advances, future trends, applications and challenges of internet of underwater things (iout): A comprehensive review. *J. Mar. Sci. Eng.* **2023**, *11*, 124. [\[CrossRef\]](#)
4. Stojanovic, M.; Preisig, J. Underwater acoustic communication channels: Propagation models and statistical characterization. *IEEE Commun. Mag.* **2009**, *47*, 84–89. [\[CrossRef\]](#)
5. Huang, J.g.; Wang, H.; He, C.b.; Zhang, Q.f.; Jing, L.y. Underwater acoustic communication and the general performance evaluation criteria. *Front. Inf. Technol. Electron. Eng.* **2018**, *19*, 951–971. [\[CrossRef\]](#)
6. Li, B.; Huang, J.; Zhou, S.; Ball, K.; Stojanovic, M.; Freitag, L.; Willett, P. MIMO-OFDM for high-rate underwater acoustic communications. *IEEE J. Ocean. Eng.* **2009**, *34*, 634–644.
7. LeCun, Y.; Bengio, Y.; Hinton, G. Deep learning. *Nature* **2015**, *521*, 436–444. [\[CrossRef\]](#)
8. Qin, Z.; Ye, H.; Li, G.Y.; Juang, B.H.F. Deep learning in physical layer communications. *IEEE Wirel. Commun.* **2019**, *26*, 93–99. [\[CrossRef\]](#)
9. Lu, H.; Jiang, M.; Cheng, J. Deep learning aided robust joint channel classification, channel estimation, and signal detection for underwater optical communication. *IEEE Trans. Commun.* **2020**, *69*, 2290–2303. [\[CrossRef\]](#)
10. Zhang, Y.; Li, J.; Zakharov, Y.; Li, X.; Li, J. Deep learning based underwater acoustic OFDM communications. *Appl. Acoust.* **2019**, *154*, 53–58. [\[CrossRef\]](#)

11. Zhang, Y.; Li, C.; Wang, H.; Wang, J.; Yang, F.; Meriaudeau, F. Deep learning aided OFDM receiver for underwater acoustic communications. *Appl. Acoust.* **2022**, *187*, 108515. [[CrossRef](#)]
12. Liu, J.; Ji, F.; Zhao, H.; Li, J.; Wen, M. CNN-based underwater acoustic OFDM communications over doubly-selective channels. In Proceedings of the 2021 IEEE 94th Vehicular Technology Conference (VTC2021-Fall), Norman, OK, USA, 27–30 September 2021; pp. 1–6.
13. Liu, L.; Cai, L.; Ma, L.; Qiao, G. Channel state information prediction for adaptive underwater acoustic downlink OFDMA system: Deep neural networks based approach. *IEEE Trans. Veh. Technol.* **2021**, *70*, 9063–9076. [[CrossRef](#)]
14. Ouyang, D.; Li, Y.; Wang, Z. Channel estimation for underwater acoustic OFDM communications: An image super-resolution approach. In Proceedings of the ICC 2021-IEEE International Conference on Communications, Montreal, QC, Canada, 14–23 June 2021; pp. 1–6.
15. Liu, S.; Mou, Y.; Wang, X.; Su, D.; Cheng, L. Denoising enabled channel estimation for underwater acoustic communications: A sparsity-aware model-driven learning approach. *Intell. Conver. Netw.* **2023**, *4*, 1–14. [[CrossRef](#)]
16. Mohan, S.; Kadkhodaie, Z.; Simoncelli, E.P.; Fernandez-Granda, C. Robust and interpretable blind image denoising via bias-free convolutional neural networks. *arXiv* **2019**, arXiv:1906.05478.
17. Zhang, Y.; Wang, H.; Tai, Y.; Li, C.; Meriaudeau, F. A machine learning label-free method for underwater acoustic OFDM channel estimations. In Proceedings of the 15th International Conference on Underwater Networks & Systems, Shenzhen, China, 22–24 November 2021; pp. 1–5.
18. Li, B.; Zhou, S.; Stojanovic, M.; Freitag, L.; Willett, P. Multicarrier Communication over Underwater Acoustic Channels with Nonuniform Doppler Shifts. *IEEE J. Ocean. Eng.* **2008**, *33*, 198–209.
19. Minn, H.; Bhargava, V.K. An investigation into time-domain approach for OFDM channel estimation. *IEEE Trans. Broadcast.* **2000**, *46*, 240–248. [[CrossRef](#)]
20. Zhang, Y.; Wang, H.; Li, C.; Chen, X.; Meriaudeau, F. On the performance of deep neural network aided channel estimation for underwater acoustic OFDM communications. *Ocean Eng.* **2022**, *259*, 111518. [[CrossRef](#)]
21. Zhang, K.; Zuo, W.; Chen, Y.; Meng, D.; Zhang, L. Beyond a gaussian denoiser: Residual learning of deep cnn for image denoising. *IEEE Trans. Image Process.* **2017**, *26*, 3142–3155. [[CrossRef](#)]
22. Kay, S.M. *Fundamentals of Statistical Signal Processing: Estimation Theory*; Prentice-Hall, Inc.: Hoboken, NJ, USA, 1993.
23. Gizzini, A.K.; Chafii, M.; Nimr, A.; Fettweis, G. Enhancing least square channel estimation using deep learning. In Proceedings of the 2020 IEEE 91st Vehicular Technology Conference (VTC2020-Spring), Antwerp, Belgium, 25–28 May 2020; pp. 1–5.
24. Moon, T.K.; Stirling, W.C. *Mathematical Methods and Algorithms for Signal Processing*; Prentice-Hall, Inc.: Hoboken, NJ, USA, 2000.
25. Hirose, A. *Complex-Valued Neural Networks*; Springer Science & Business Media: Berlin/Heidelberg, Germany, 2012; Volume 400.
26. Guberman, N. On complex valued convolutional neural networks. *arXiv* **2016**, arXiv:1602.09046.
27. Huang, S.; Yang, T.; Huang, C.F. Multipath correlations in underwater acoustic communication channels. *J. Acoust. Soc. Am.* **2013**, *133*, 2180–2190. [[CrossRef](#)]
28. Qiao, G.; Song, Q.; Ma, L.; Liu, S.; Sun, Z.; Gan, S. Sparse Bayesian learning for channel estimation in time-varying underwater acoustic OFDM communication. *IEEE Access* **2018**, *6*, 56675–56684. [[CrossRef](#)]
29. Zhou, Y.h.; Tong, F.; Zhang, G.q. Distributed compressed sensing estimation of underwater acoustic OFDM channel. *Appl. Acoust.* **2017**, *117*, 160–166. [[CrossRef](#)]

**Disclaimer/Publisher’s Note:** The statements, opinions and data contained in all publications are solely those of the individual author(s) and contributor(s) and not of MDPI and/or the editor(s). MDPI and/or the editor(s) disclaim responsibility for any injury to people or property resulting from any ideas, methods, instructions or products referred to in the content.